

Performance of Multilayered Thermophotovoltaic Elements at Moderate Temperature

Linda Z. Shi* and R. F. Boehm†

University of Nevada, Las Vegas, Las Vegas, Nevada 89154-4027

An analysis of stacked thermophotovoltaic elements at moderate temperature is reported. The motivation is for application to microsystems. Various numbers of layers are considered, with a variety of temperatures (varying from 560 to 360 K) on the higher-temperature end. At the lower-temperature end, the temperature is always held at 300 K. It is assumed that the photovoltaic (PV) material is thin, but the thickness is considered. The PV material investigated in an earlier single-layer study ($\text{In}_{0.8}\text{Ga}_{0.2}\text{As}$) is considered, as well as $\text{Hg}_{0.8}\text{Cd}_{0.2}\text{Te}$. The latter demonstrates absorption and PV conversion at longer wavelengths than the former. In all cases, the emitter surface of the TPV pair is taken to be black. It is shown that both the power output and the efficiency of the system increase with layering.

Nomenclature

c_0	=	speed of light in a vacuum, 3.0×10^8 m/s
$E_{\lambda,bi}$	=	blackbody emissive power of i th layer, $\text{W}/\mu\text{m} \cdot \text{m}^2$
E_g	=	bandgap energy, eV
e	=	electron charge, -1.602×10^{-19} C
h	=	Planck's constant, 6.626×10^{-34} J s
I_d	=	dark saturation current of the last layer, A/m^2
$I_{sc,i}$	=	short-circuit current of i th layer, A/m^2
K_b	=	Boltzmann's constant, 1.381×10^{-23} J/K
k, k_λ	=	extinction coefficient
k	=	thermal conductivity of photovoltaic (PV) material, $\text{W}/\text{m} \cdot \text{K}$
L	=	thickness of intervening material layer, m
n, n_λ	=	refractive index
P	=	electrical power output, W/m^2
$q_{cond,i}$	=	conduction heat flux of the i th layer of PV material, W/m^2
$q_{net,i}$	=	net heat transfer of the i th layer, W/m^2
$q_{\lambda 0,i}$	=	spectral radiosity of the i th layer, $\text{W}/\mu\text{m} \cdot \text{m}^2$
T_H	=	the highest temperature in the stack, K
T_i	=	higher temperature of the i th slab of PV material, K
T_i'	=	lower temperature of the i th slab of PV material, K
T_L	=	lowest temperature in the stack, always taken to be 300 K
$V_{oc,i}$	=	open-circuit voltage of i th layer, V
x	=	fraction of Ga in InGaAs or of Cd in HgCdTe
ε_λ	=	monochromatic emissivity
η	=	overall stack power generation efficiency, defined as the total power generated divided by the heat transfer across the first gap
$\eta_{PV\lambda}$	=	monochromatic external quantum efficiency of PV material
λ	=	wavelength, μm
$\lambda_{f,i}$	=	upper limit of the wavelength for the i th layer, μm
$\lambda_{i,i}$	=	lower limit of the wavelength for the i th layer, μm
ν	=	quantity defined in Eq. (11b)

Introduction

THERMOPHOTOVOLTAIC (TPV) systems have been an object of study for several decades. Virtually all of the attention has been directed to high-temperature-difference systems. Some of this work has been reviewed in a companion paper.¹

Received 22 December 2000; revision received 25 June 2001; accepted for publication 26 June 2001. Copyright © 2001 by the American Institute of Aeronautics and Astronautics, Inc. All rights reserved.

*Graduate Research Assistant, Mechanical Engineering.

†Director, Center for Energy Research, Box 454027, Howard R. Hughes College of Engineering.

In this study attention is directed to moderate temperature systems. Specifically, this is motivated by the possibility that the TPV approach might be applicable to power generation in microdevices. In these kinds of systems, very high-temperature differences, as are characteristically sought to maximize power generation in TPV systems, cannot be tolerated because of the very small dimensions involved. For this reason, temperatures up to 560 K are chosen for the hot side, and the cold side temperature is always assumed to be 300 K.

In a companion paper,¹ the characteristics of two distinct single-layer systems using $\text{In}_{0.8}\text{Ga}_{0.2}\text{As}$ PV material were examined. In all cases, the net power was very small, quite characteristic of the moderate temperatures considered.

Now consider the situation when TPV pairs are stacked. Of particular interest is to quantify the effect of layering on both the power output and the efficiency. One of the systems examined previously [gray emitter with a $\text{In}_{0.8}\text{Ga}_{0.2}\text{As}$ photovoltaic (PV) material] is considered here, with the initial emitter surface taken as black. The effect of a smaller bandgap material ($\text{Hg}_{0.8}\text{Cd}_{0.2}\text{Te}$) is also evaluated to see what effect this may have.

Note that details of the actual PV construction, and their effects on the performance of the system, are not considered here. One of several forms of surface treatment will be required to allow the PV current to be harvested. Conceptually the same analysis as will be described subsequently would be used to account for these factors, albeit with undoubtedly modified parameters.

Analysis

It is assumed that all system pairs, except for the first, are constructed of the same material. The first pair is assumed to consist of a gray emitter exchanging energy with the PV material. Furthermore, this system is assumed to be parallel and infinite. The spacing between the pairs is large compared to the wavelength of the radiation, but there are no edge losses. Radiation is the only mode of transfer between the pairs, and the form factor between the surfaces is taken as unity. Once the radiation is absorbed by the PV material, however, some power is generated as dictated by the quantum efficiency. The remainder of the absorbed energy is conducted through the PV material to be emitted on the opposite side from where it was absorbed.

A diagram of the system considered is shown in Fig. 1. The basic calculation approach is described in what follows.

First the spectral, blackbody emissive power of i th layer is written using the Planck function (see Ref. 2):

$$E_{\lambda,bi} = \frac{2\pi hc_0^2}{\lambda^5 [\exp(hc_0/\lambda K_b T_i') - 1]} \quad (1)$$

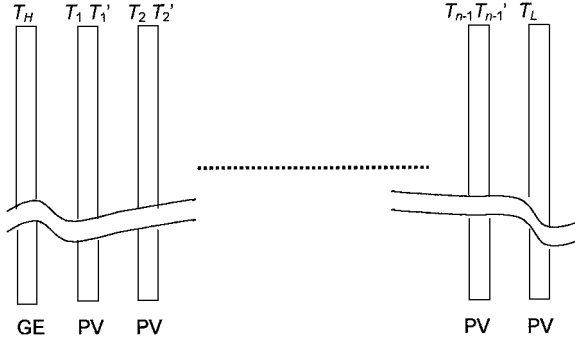


Fig. 1 System made up of a stack of PV surface pairs, except the first surface, which is taken to be a gray emitter.

In this equation, $i = 1, 2, \dots, n$, and $T'_0 = T_H$.

Then the spectral net heat transfer between two surfaces is found²

$$q_{\lambda i} = \frac{E_{\lambda, b(i-1)} - E_{\lambda, bi}}{[1/\varepsilon_{\lambda(i-1)} + 1/\varepsilon_{\lambda i} - 1]} \quad (2)$$

In the cases discussed here, the optical constants (n and k) will be known, and the emissivity is calculated from those values. The monochromatic result used is one from electromagnetic theory and is given as² follows:

$$\begin{aligned} \varepsilon_{\lambda} = & 4n_{\lambda} - 4n_{\lambda}^2 \ell n \frac{1 + 2n_{\lambda} + n_{\lambda}^2 + k_{\lambda}^2}{n_{\lambda}^2 + k_{\lambda}^2} \\ & + \frac{4n_{\lambda}(n_{\lambda}^2 - k_{\lambda}^2)}{k_{\lambda}} \tan^{-1} \left(\frac{k_{\lambda}}{n_{\lambda}^2 + k_{\lambda}^2} \right) + \frac{4n_{\lambda}}{n_{\lambda}^2 + k_{\lambda}^2} \\ & - \frac{4n_{\lambda}^2}{(n_{\lambda}^2 + k_{\lambda}^2)^2} \ell n (1 + 2n_{\lambda} + n_{\lambda}^2 + k_{\lambda}^2) \\ & - \frac{4n_{\lambda}(-n_{\lambda}^2 + k_{\lambda}^2)}{k_{\lambda}(n_{\lambda}^2 + k_{\lambda}^2)^2} \tan^{-1} \frac{k_{\lambda}}{1 + n_{\lambda}} \end{aligned} \quad (3)$$

For this equation to hold, the square of the sine of the angle of incidence has to be less than the sum of the squares of the optical constants. This is found to be the case over virtually all wavelengths.

Irradiation on the PV surface, needed for calculating the power production, is found from the radiosity of the opposing surface in the infinite parallel plate geometry,²

$$q_{\lambda, oi} = E_{\lambda, b(i-1)} - [(1 - \varepsilon_{\lambda i})/\varepsilon_{\lambda i}] q_{\lambda i} \quad (4)$$

Open-circuit current for the PV material can be found from the quantum efficiency and the irradiation. See further discussion of this formulation in Ref. 1.

$$I_{sc, i} = \frac{e}{hc} \int_{\lambda_{i, i}}^{\lambda_{f, i}} \lambda \eta_{PV \lambda} q_{\lambda, oi} d\lambda \quad (5)$$

In turn, the dark current at 300 K can be calculated as³

$$I_d = 1.5 \times 10^9 \exp(-Eg/K_b T_L) \quad (6)$$

where

$$\begin{aligned} Eg(x, T) = & -0.302 + 1.93x + 5.35 \times 10^{-4} T(1 - 2x) \\ & - 0.810x^2 + 0.832x^3 \end{aligned} \quad (7)$$

for $\text{Hg}_{1-x}\text{Cd}_x\text{Te}$ (Ref. 4) and

$$Eg = 0.35 + 0.5x + 0.59x^2 \quad (8)$$

for $\text{In}_{(1-x)}\text{Ga}_x\text{As}$ (Ref. 5).

Next, the open-circuit voltage for the PV material at $T = 300$ K can be found,³

$$V_{oc, n} = (K_b T_L / e) \ell n (I_{sc, n} / I_d + 1) \quad (9)$$

All PV surfaces in the stack except the lowest temperature one will be at temperatures above 300 K. Because the open-circuit voltage

decreases at a rate of about 0.2% with each degree of temperature increase,³ this variation can be written as

$$V_{oc, i} = [1 - 0.002(T_i - 300)] V_{oc, n} \quad i = 1, 2, \dots, n-1 \quad (10)$$

Then the fill factor (FF) of the i th layer can be determined³

$$FF_i = \frac{v_i - \ell n(v_i + 0.72)}{v_i + 1} \quad (11a)$$

where

$$v_i \equiv \frac{V_{oc, i}}{K_b T_i / e} \quad (11b)$$

At this point the power output for the complete assembly can be found by summing up the individual contributions from each surface:

$$P_{\text{total}} = \sum_{i=1}^n P_i = \sum_{i=1}^n I_{sc, i} V_{oc, i} FF_i \quad (12)$$

Now consider the heat transfer per unit area between layers, which is assumed to be by conduction,

$$q_{\text{cond}, i} = k[(T_i - T'_i)/L] \quad (13)$$

Note that the radiation between two surfaces can be found by integrating Eq. (1) over all wavelengths. An energy balance is then used to determine the intermediate temperatures:

$$q_i - q_{(i+1)} = P_i \quad (14)$$

$$q_{\text{cond}, i} = q_{i+1} \quad (15)$$

In essence these two equations represent the assumption that the power is generated at the surface of the cooler surface, removing that amount of energy from further interaction with the stack. The energy that remains at that point is then assumed to be conducted through the lower-temperature material, where it becomes the radiative transport for the next lower-temperature pair (convection is assumed to be absent). This allows the temperature on each surface of each layer to be determined.

The number of unknown variables is reduced by expanding Eq. (13) to express T_i in terms of T'_i , T_H , and T_L :

$$T_i = T'_i + (L/k) q_{i+1} \quad (16)$$

At this point, the power generation efficiency can be found,

$$\eta = P_{\text{total}} / q_1 \quad (17)$$

where the radiative heat transfer is the total value found over all wavelengths:

$$q = \int_0^\infty q_{\lambda} d\lambda \quad (18)$$

In this work, the lowest-temperature layer T_L is always taken to be 300 K, and the highest-temperature in the stack, T_H , is taken variously to be 560, 460, and 360 K. Two PV materials are studied. One is $\text{In}_{0.8}\text{Ga}_{0.2}\text{As}$, and the other is $\text{Hg}_{0.8}\text{Cd}_{0.2}\text{Te}$. The reason for choosing $\text{In}_{0.8}\text{Ga}_{0.2}\text{As}$ is to compare results with Ref. 1. $\text{Hg}_{0.8}\text{Cd}_{0.2}\text{Te}$ was chosen for comparison here because the effective quantum efficiency wavelength range for this material is 8–12 μm . These wavelengths correspond more closely to the wavelength of the maximum value of spectral emissive power at moderate temperature, according to Wien's displacement law.

Properties of $\text{In}_{0.8}\text{Ga}_{0.2}\text{As}$

The spectral emissivity and quantum efficiency for this material were described previously.¹ These variations are shown in Fig. 2 for comparison to other properties to be introduced later. Tabulations of the emissivity over a wider wavelength range are given in Ref. 1.

Properties of $\text{Hg}_{0.80}\text{Cd}_{0.20}\text{Te}$

Spectral Emissivity

The same approach as was used in Ref. 1 is used here to compute the spectral hemispherical emissivity. To do this, the optical

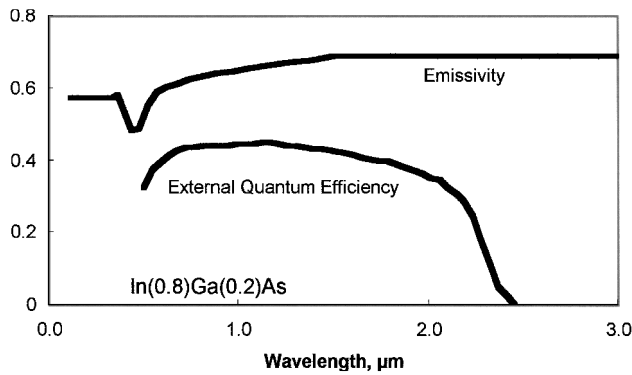


Fig. 2 External quantum efficiency and emissivity for the same wavelength range of interest for $\text{In}_{0.8}\text{Ga}_{0.2}\text{As}$ (Ref. 1).

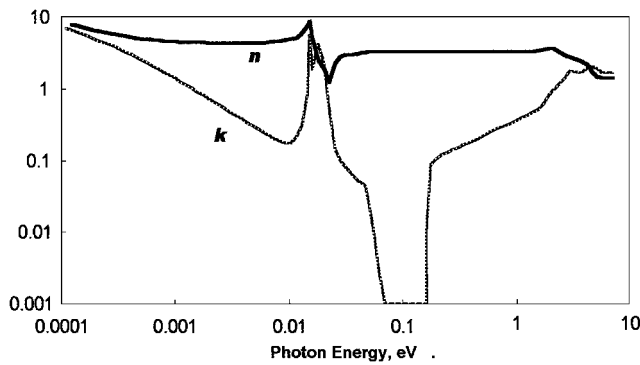


Fig. 3 Refractive index n and extinction coefficient k of $\text{Hg}_{0.8}\text{Cd}_{0.2}\text{Te}$ (adapted from Whale⁵).

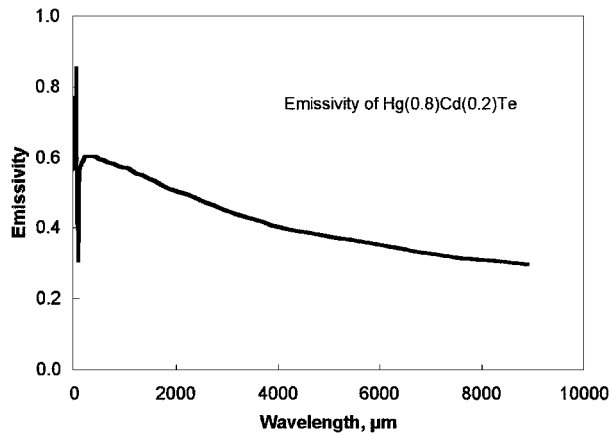


Fig. 4 Emissivity of $\text{Hg}_{0.8}\text{Cd}_{0.2}\text{Te}$ over a broadband of wavelengths as calculated from Eq. (3).

properties shown in Fig. 3 are used.^{5,6} They are then used with Eq. (3) to find the emissivity. Variation of this property is shown in Fig. 4 over a very broad range of wavelength. In Fig. 5, details of the emissivity variation in the pertinent range near the bandgap for this material are shown.

Spectral Quantum Efficiency

This material has been of interest to the scientific community for application in infrared (IR) detectors, but has not been considered to any extent for TPV applications. As a result the quantum efficiency has not been of particular interest to researchers. Limited data can be found in the literature. For example, a value of 0.27 is tabulated by Jones et al.⁷ for higher temperature (compared to liquid nitrogen temperatures) IR detector applications. With sensitivity to radiation in the range between 5 and 12 μm , this material has a great deal of utility for this application. In lieu of more definitive

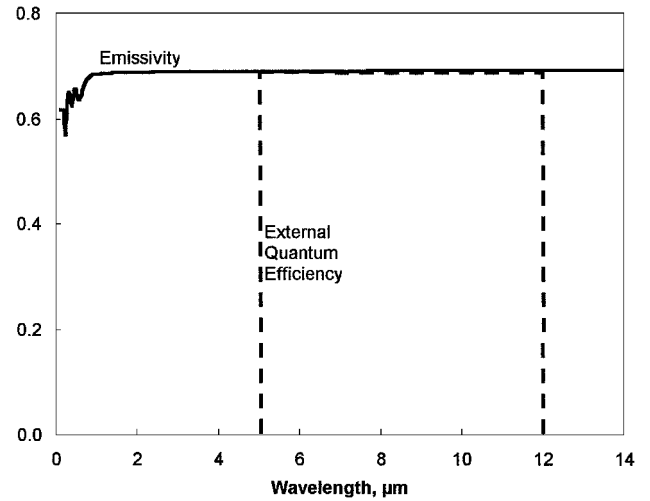


Fig. 5 Calculated emissivity and assumed external quantum efficiency variation of $\text{Hg}_{0.8}\text{Cd}_{0.2}\text{Te}$.

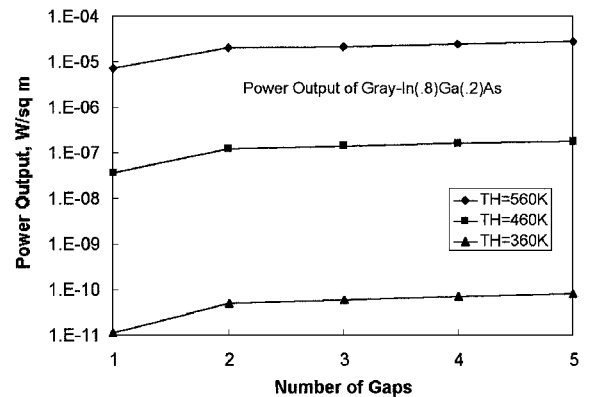


Fig. 6 Power output from multilayer systems of $\text{In}_{0.8}\text{Ga}_{0.2}\text{As}$; results for three separate highest temperatures with lowest temperature 300 K in all cases.

information, we assume that the material demonstrates the maximum possible spectral quantum efficiency. That is, the quantum efficiency is the same value at each wavelength as is the absorptivity (clearly no more power can be generated than radiosity absorbed), which on a monochromatic basis is the same value as the emissivity. On a monochromatic basis, the assumed variation for the spectral quantum efficiency is shown in Fig. 5. This approximation is used throughout the evaluations reported here.

Solution Approach

Routines within the MATLAB[®] 5.3 libraries were used for the numerical evaluation of the system described. In the software, the function for integration is QUAD. This involves an adaptive recursive Simpson's Rule routine with a specified relative error. A constrained optimization routine was then used to minimize the errors in the energy balances at each surface in the stack. This was accomplished by using trial values of the various temperatures in the system. When the errors were close enough to zero, the optimization solution was concluded. Throughout, the optimization was constrained such that the subsequent layer temperatures decrease in value. Hence,

$$T_H > \dots > T_i \dots > T_L \quad (19)$$

In addition to determining the temperature of each of the surfaces in the stack, the heat flows and powers generated were also found.

Results and Discussion

Calculations for power generation related to the $\text{In}_{0.8}\text{Ga}_{0.2}\text{As}$ multilayered system are shown in Fig. 6. The effect of the additional

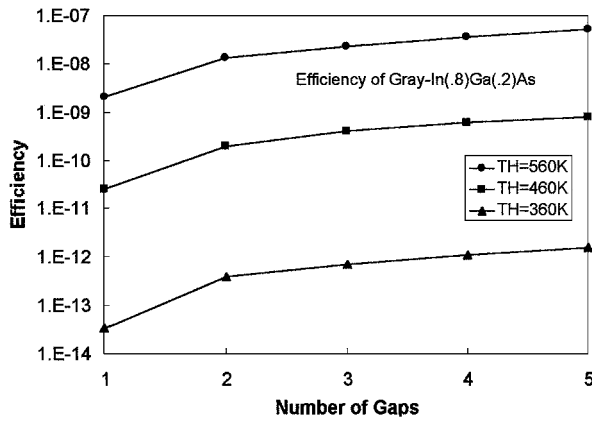


Fig. 7 System efficiency for multilayer systems of $\text{In}_{0.8}\text{Ga}_{0.2}\text{As}$; results for three separate highest temperatures with lowest temperature 300 K in all cases.

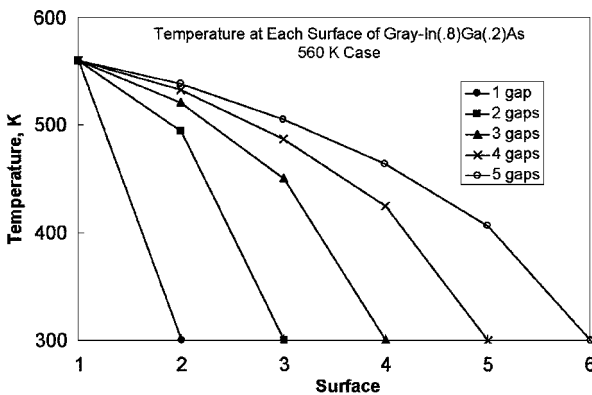


Fig. 8 Temperatures of each of the surfaces for a $\text{In}_{0.8}\text{Ga}_{0.2}\text{As}$ system for highest temperature of 560 K and lowest temperature of 300 K.

layers shows an increase in power output over the single gap base. Approximately 800% increase over the maximum number of layers investigated here is shown for the lowest-temperature case. This decreases with increasing temperature to something less than 400% at the highest-temperature case. This demonstrates the relative greater importance of the radiation from the lower-temperature surfaces in the lowest-temperature case. However, the overall increase in power level with temperature for all situations is clearly undeniable.

When the power values shown in Fig. 6 are ratioed to the net heat transfer across the first gap, the result is the overall efficiency for the system. This is shown in Fig. 7. Similar trends to Fig. 6 are obviously seen here. Even more significant improvements over the single-gap case are demonstrated for the efficiency compared to the power generation. This is a result of the increased power output and the decreased heat transfer associated with more layers.

Figure 8 shows the corresponding surface temperatures that yielded the values shown in Figs. 6 and 7, for the highest-temperature case (560–300 K). Note that these results are for a very thin PV layer (small L), and this yields the two surfaces of a given slab of material at almost the same temperature. This does not have to be the case with the model formulated, but the effects of a lesser number of parameters can be examined this way.

Results for power output for the multilayered case with $\text{Hg}_{0.8}\text{Cd}_{0.2}\text{Te}$ as the PV material are shown in Fig. 9. Note that these are significantly higher power outputs compared to the $\text{In}_{0.8}\text{Ga}_{0.2}\text{As}$ case that is shown in Fig. 6. The general increase varies from four orders of magnitude in the higher-temperature case to over eight orders of magnitude in the lower-temperature case.

Efficiencies for the $\text{Hg}_{0.8}\text{Cd}_{0.2}\text{Te}$ system are shown in Fig. 10. As in the case of InGaAs , they mirror the corresponding power generation situation. Again, the efficiency increases more markedly than does the power generation. This is due to the increasing power

Table 1 Results for multigap calculations in the black $\text{Hg}_{0.8}\text{Cd}_{0.2}\text{Te}$ system^a

Gaps	Power W/m^2	Efficiency $\times 10^3$	Power increase over one gap, %	Efficiency increase over one gap, %
1	0.414	0.117	—	—
2	0.991	0.647	139	453
3	1.19	1.22	187	943
4	1.43	2.00	245	1620
5	1.69	2.99	308	2460

^aAll cases are for $T_H = 560$ K and $T_L = 300$ K.

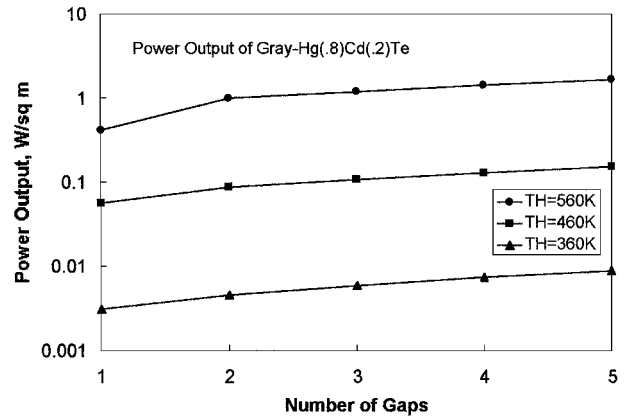


Fig. 9 Power output from multilayer systems of $\text{Hg}_{0.8}\text{Cd}_{0.2}\text{Te}$; results for three separate highest temperatures with lowest temperature 300 K in all cases.

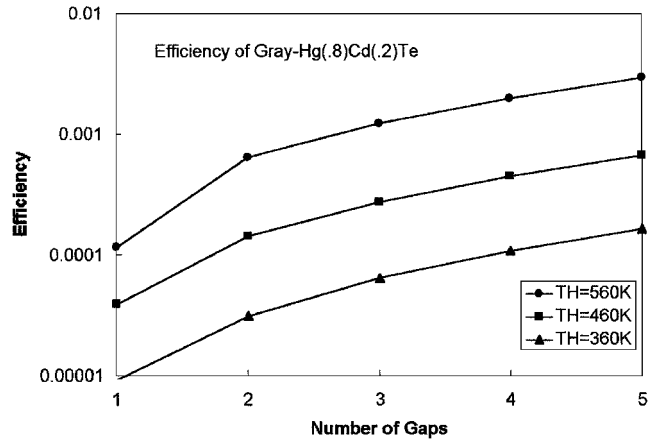


Fig. 10 System efficiency for multilayer systems of $\text{Hg}_{0.8}\text{Cd}_{0.2}\text{Te}$; results for three separate highest temperatures with lowest temperature 300 K in all cases.

generation and the decreasing heat flux with larger numbers of gaps. Note that the values are at least four orders of magnitude higher in Fig. 10 compared to Fig. 7. Less spread is shown between the higher-temperature case and the lower-temperature case in Fig. 10 compared to Fig. 7.

Increases in both the power generation and efficiency are shown to be substantial. These are compared directly in Table 1.

In Fig. 11 the surface temperatures for the highest-temperature $\text{Hg}_{0.8}\text{Cd}_{0.2}\text{Te}$ case is shown. Little difference in the temperature variation for this case is shown compared to Fig. 8.

Generally, the layering of PV pairs exhibits two effects that are in opposition. One is that several of the surfaces in a layered system are at a higher temperature than the 300-K base that was assumed throughout. The increase in temperature decreases the open circuit voltage. This in turn decreases PV cell power output (all other things being equal). The net result is a negative effect on power output. However, the reemitting of the radiation at only slightly decreased (due to decreased temperature) levels at each layer offers more sources

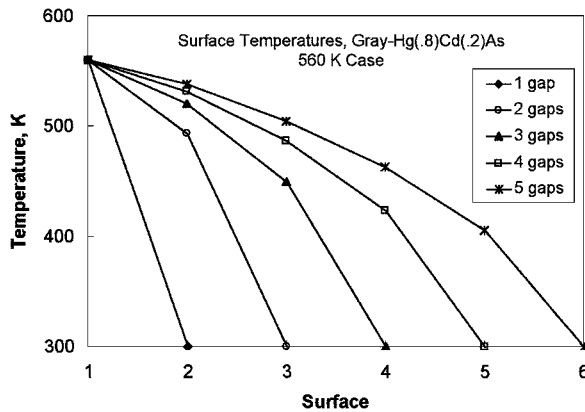


Fig. 11 Temperatures of each of the surfaces in a $\text{Hg}_{0.8}\text{Cd}_{0.2}\text{Te}$ system for the highest-temperature case (560 K).

of power generation only slightly less directly proportional to the number of gaps. This has an increasing effect on power output. As can be seen from the results, though, the net result is to increase the power generated and system efficiencies with layering.

In the studies carried out here, the thickness of the PV material was taken to be small (0.0001 m throughout). This decreased the temperature drop between pairs as a result of decreasing conduction resistance compared to thicker materials. However, small PV thickness could also affect the electrical power generated. The impact of this is not included in this analysis.

A black emitter was used throughout this analysis, which will maximize the power output. Efficiency values for either material could be increased by use of an ideal selective surface.¹

Clearly the power outputs from these types of systems are very low, primarily due to the temperature levels assumed in the analysis. An effect, not included here, that may have a large, positive influence on the results is that of close spacings. It is known that radiative transfer between two surfaces can be greatly enhanced when the surface spacing is smaller than the characteristic wavelength of the radiation.^{5,8} This effect will be the focus of later work.

Conclusions

1) An analysis of multilayered TPV systems has been carried out. This has been done at moderate temperatures for possible microdevice applications.

2) Two different PV material cases have been considered, one using an InGaAs compound and the other using a form of HgCdTe . The InGaAs material was chosen to compare to an earlier paper considering that material for a single-gap arrangement. $\text{Hg}_{0.8}\text{Cd}_{0.2}\text{Te}$ was chosen for comparison purposes because of its small bandgap characteristics.

3) Radiation is assumed as the only heat transfer mode across gaps, and simple conduction is taken across each material layer. For this analysis, the material thickness is taken to be small.

4) To determine the temperatures of the system, an optimization calculation was performed that minimized the error in an energy balance at each surface.

5) It was found that the energy produced increased substantially with layering of gaps and surfaces, up to 308% compared to the one-layer case for $\text{Hg}_{0.8}\text{Cd}_{0.2}\text{Te}$.

6) The power generation efficiency (defined as the power generated divided by the heat transfer across the first gap) increased even more than the power generated. Increases up to 2460% were seen for the $\text{Hg}_{0.8}\text{Cd}_{0.2}\text{Te}$ cases examined.

7) Overall energy production is quite small, primarily due to the small temperature levels assumed in the analysis. Effects of the enhancement of radiative transfer due to small spacing of the surfaces needs to be evaluated.

References

- ¹Shi, L. Z., Xu, S. Y., and Boehm, R. F., "Analysis of a Single-Layer Thermophotovoltaic System at Moderate Temperatures," *Journal of Thermophysics and Heat Transfer*, Vol. 15, No. 4, 2001, pp. 453-457.
- ²Seigel, R., and Howell, J., *Thermal Radiation Heat Transfer*, 3rd ed., Hemisphere, New York, 1992, pp. 22, 121, 334.
- ³Green, M. A., *Solar Cells: Operating Principles, Technology, and System Applications*, Prentice-Hall, Englewood Cliffs, NJ, 1982, Chaps. 4, 5.
- ⁴Hansen, G. L., Schmit, J. L., and Casselman, T. N., "Energy-Gap vs Alloy Composition in $\text{Hg}_{1-x}\text{Cd}_x\text{Te}$," *Journal of Applied Physics*, Vol. 53, No. 10, 1982, pp. 7099-7101.
- ⁵Whale, M. D., "Fluctuational Electrodynamics Analysis of Microscale Radiative Transfer and the Design of Microscale Thermophotovoltaic Devices," Ph.D. Dissertation, Massachusetts Inst. of Technology, Cambridge, MA, 1997.
- ⁶Amirtharaj, P. M., "Mercury Cadmium Telluride," *Handbook of Optical Constants of Solids II*, Academic Press, San Diego, CA, 1991, pp. 655-689.
- ⁷Jones, C. L., Matthews, B. E., Purdy, D. R., and Metcalfe, N. E., "Fabrication and Assessment of Optically Immersed CdHgTe Detector Arrays," *Semiconductor Science and Technology*, Vol. 6, 1991, pp. C110-C113.
- ⁸Boehm, R. F., and Tien, C. L., "Small Spacing Analysis of Radiative Transfer Between Parallel Metallic Surfaces," *Journal of Heat Transfer*, Vol. 92, No. 3, 1970, pp. 405-411.